Determination of the Elastic Modulus of the Coating Using a Spherical Indenter

B.A. Garibyan[1]

[1]Moscow Aviation Institute (National Research University), Volokolamskoe shosse, 4, 125993, Moscow, Russia
[1]bagarib@yandex.ru

Abstract : In this work, we investigate the nanoindentation of the surface of powder paint and varnish coatings on an epoxy-polyester base, applied to steel substrates. The study of the influence of the test method on the identified mechanical properties has been carried out. A comparison is made of the measurement results obtained using a spherical indenter and a Berkovich indenter. Estimates of the reduced modulus of elasticity, Young's modulus and hardness of coatings are obtained. The obtained experimental data indicate a significant dependence of the determined mechanical properties of paint and varnish coatings depending on the type of indenter used. In the case of using the Berkovich indenter, the found Young's modulus of the coatings (0,6 GPa) turns out to be underestimated in relation to the properties of coatings known from macro experiments (3 GPa). When using a spherical indenter, Young's modulus turns out to be overestimated (6,3 GPa).

1. Introduction

In recent years, the continuous indentation method, previously known as the kinetic hardness method, has been increasingly used to determine the hardness of materials and coatings [1-4]. The essence of the kinetic hardness method lies in the fact that an indenter is embedded in the material under study and at the same time two parameters are recorded: the load and the depth of penetration of the indenter. Hardness is defined as the quotient of the load divided by the surface area of the print or its projection. Currently, EU standards also provide for kinetic indentation for hardness determination, while adhering to the following hardness determination levels:

1. macrolevel: 2 H < P < 30000 H,
2. microlevel: P < 2 H, h > 200 nm,
3. nanolevel: h < 200 nm, P < 2 мН

where P - load, h - indentation depth.

It is quite obvious that the 1st level is most consistent with the generally accepted term macrohardness, the 2nd level is microhardness, and the 3rd level is logically called nanohardness.

The basic principles of the analytical model used in the indentation method are [5-13]:

– deformation during unloading fully elastic;

– the relationship between the stiffness of the sample and the indenter can be obtained as follows:

$$\frac{1}{E_r} = \frac{1-\nu_i^2}{E_i} - \frac{1-\nu_s^2}{E_s}, \tag{1}$$

where ν_s – Poisson's ratio of the sample, ν_i – Poisson's ratio indenter, E_s – sample modulus, E_i – modulus of elasticity of the indenter, E_r – reduced module.

– contact can be modeled according to an analytical model describing the contact between a rigid indenter of a certain shape with a homogeneous isotropic elastic surface:

$$S = \frac{2\sqrt{A}}{\sqrt{\pi}} E_r, \tag{2}$$

where S – contact stiffness, A – contact area.

It was shown that this equation works for indenters of various geometries and shapes.

The essence of the method is to obtain a load-deformation relationship when a physically and geometrically certified indenter is introduced into a sample. The applied force is several millinewtons with a resolution of several nanonewtons, the deformations are several nanometers (tens of nanometers) with a resolution of up to 0,04 nm, hence the term nanoindentation.

Additional Experiment Features:

- scanning - sample movement under load (scratch test)
- shock impact - oscillation of the sample under constant load

Nanoindentation is a method that allows one to determine the mechanical and fatigue properties of various films, coatings and materials at the nanoscale. Tests at very small deformations and comparison of the obtained data with micro- and macro-experiments allow us to draw a conclusion about the relationship between the nanostructure of materials and their properties at the macrolevel.

In this work, we compare various methods of indenting polymer coatings on steel substrates with the measurement results. For the coatings under study, macro tests were previously carried out to determine the elastic modulus in bending of steel substrates with coatings [14-29]. It was shown here that the coatings, despite their small thickness, have a significant effect on the elastic properties of specimens in the form of thin steel plates. In other works, polymer coatings on the surface of other materials were created and studied [30-51]. In the experiments, the thickness of the coatings was 0.200 mm, and the thickness of the steel plates was 0,7-1,5 mm. It was shown that under bending the elastic modulus of thin plates is stably lower than the elastic modulus of thicker plates. This effect is theoretically confirmed within the framework of the classical model of an elastic three-layer beam with relatively soft outer layers (coating) and a hard middle layer (steel substrate). As a result of this experimental and theoretical study, it was found that the modulus of elasticity of the studied epoxy-polyester coatings is, on the order of 3 GPa.

In this work, the task is to verify the results obtained using the method of nanoindentation of the coating surface. This method makes it possible to quite accurately determine even the bulk (and not only surface) properties of the material, if a sufficiently large indentation force is used and if the material is homogeneous near the surface. For example, the elastic properties of grains in silicon carbide ceramics were previously measured and the Young's modulus was obtained close (within the measurement error) to the theoretically known value of Young's modulus of SiC crystals. In this work, we investigate a compliant polymer coating. It is likely that the elastic properties of this coating from indentation tests are rather difficult to estimate, due to the nonlinearity of the constitutive relations that are characteristic of this type of materials. As a result, the measurement error may arise not only due to variations in the properties of experimental samples or due to the error of the measuring equipment, but also due to a significant increase in the error of the applied Oliver-Pharr formula (1).

2. Procedure for conducting and processing the results of the experiment

The studies were carried out on samples representing rectangular steel plates 5x10 mm, on which powder polymer paint AKZO NOBEL (Holland) was applied on an epoxy-polyester basis. Coating was carried out in a Gema chamber (Switzerland) by electrostatic spraying. The color range of powder paints was selected according to the international RAL catalog. All of 4 samples were prepared with RAL 9005 (black) coating. For the experiments, the measuring complex NanoTest 600 (England).

The working body of the NanoTest 600 complex is a pendulum, which rotates on a friction-free hinge. The pendulum is lightweight and stiff enough with the maximum applied force (500 mN). The pendulum rod is made of ceramic, has a cylindrical shape; an induction coil is installed at the end of the pendulum. Under the action of an electric current, the coil moves towards the magnet, setting the law of motion of the diamond indenter towards the sample. The displacement of the indenter is measured by a capacitive sensor. The depth of penetration of the diamond indenter into the sample is specified with an error of 0,04 nm. The experiment with the NanoTest 600 was carried out according to the following procedure. The sample was fixed to the substrate using glue, then the sample was brought to the indenter. After installing the sample in the holder of the experimental complex, the surface is treated with a piezoprofilometer. This is necessary to determine the geometry of the surface on which the indentation is carried out. The results are shown in Fig. 1, but the examination surface is at an angle to the holder. This did not affect the course of the experiment, since the dimensions of the indenter are many times smaller than the inclined platform. We can assume that contact occurs at the point.
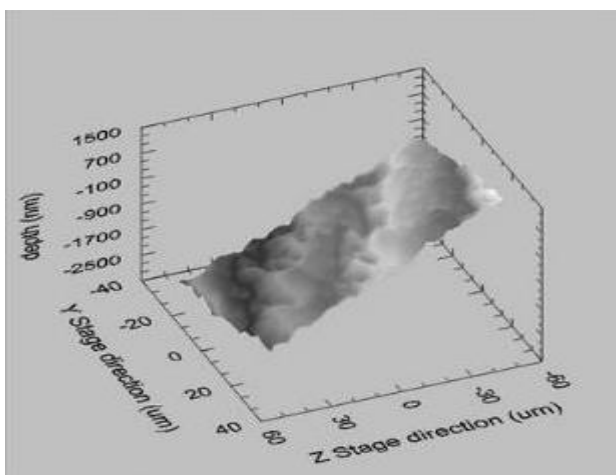
Figure: 1. Topography of the sample coating surface.

Sample indentation was carried out at 10 points with an interval of 20-30 μm. The load was increased at a constant rate of 0,05 mN/s until a given maximum load of 10 mN was reached when using a Berkovich indenter and up to 50 mN when using a spherical indenter. This choice of load is justified by the different contact area of the indenters. In this experiment, a Berkovich indenter with an apex angle of 65,3º and a radius of curvature of 200nm was used. The radius of the spherical indenter was 10 μm. The indentation rate was set on the assumption that the load cycle should take 20 s.

Based on the experimental data obtained, the computer system of the NanoTest 600 complex automatically calculated a number of parameters: maximum penetration depth, plastic deformation, hardness, reduced modulus, elastic recovery, contact compliance, plastic work, elastic work, and others. When calculating the reduced modulus (modulus of elasticity of the sample + indenter system), the Oliver - Pharr model is used, in accordance with which a part of the load – penetration depth dependence is described during unloading. The accompanying software based on the Oliver-Pharr model calculates the permanent plastic deformation h_c, hardness H and reduced modulus E_r.

Plastic deformation h_c is determined from the equation:

$$h_c = h_{max} - \varepsilon(CP_{max}), \tag{3}$$

where C – it is the compliance of the contact (equivalent to the tangent of the slope of the unloading curve at maximum load). The value of ε depends on the geometry of the indenter, for indenter Berkovich $\varepsilon = 0,75P_{max}$ – maximum load, h_{max} – maximum penetration depth of the indenter.

The function of the dependence of the contact area on the immersion depth A (h_c) is determined when the device is calibrated on a special calibration sample - quartz.

Hardness H is determined based on the maximum load P_{max} and the contact area of the indenter with the sample A:

$$H = \frac{P_{max}}{A}. \tag{4}$$

To calculate the reduced modulus of elasticity of the sample, a part of the curve is processed during unloading in accordance with the relation:

$$C = \frac{dh}{dP} = \frac{\sqrt{\pi}}{2E_r\sqrt{A}}, \tag{5}$$

Thus, knowing the value of E_r - the reduced modulus, which the device determines from relation (5) when processing experimental data, using equation (1) it is possible to calculate the elastic modulus of the sample or film on the sample surface. For calculations, we need to know the Poisson ratio of the coverage, which we take equal to 0.33. A change in this value within 0.2-0.4, in principle, insignificantly affects the measurement results.

3. Measurement results

When nanoindentation of paint and varnish coatings using a Berkovich indenter with a load of 10 mN, the maximum penetration depth of the indenter into the coating is 6 μm. When using a spherical indenter with a load of 50 mN, the maximum penetration was 5 μm. The obtained indentation depth makes it possible to minimize the influence of both the sample surface roughness (up to 1 μm) and a more elastic substrate (coating thickness 200 μm) on the obtained load-deformation dependences. Thus, the experimental results characterize exclusively the mechanical properties of the coating material, which is also evidenced by the small scatter of the obtained experimental data (Table 1, Fig. 2).

Table 1. Test results for powder-coated specimens (in parentheses, the standard deviation is given).

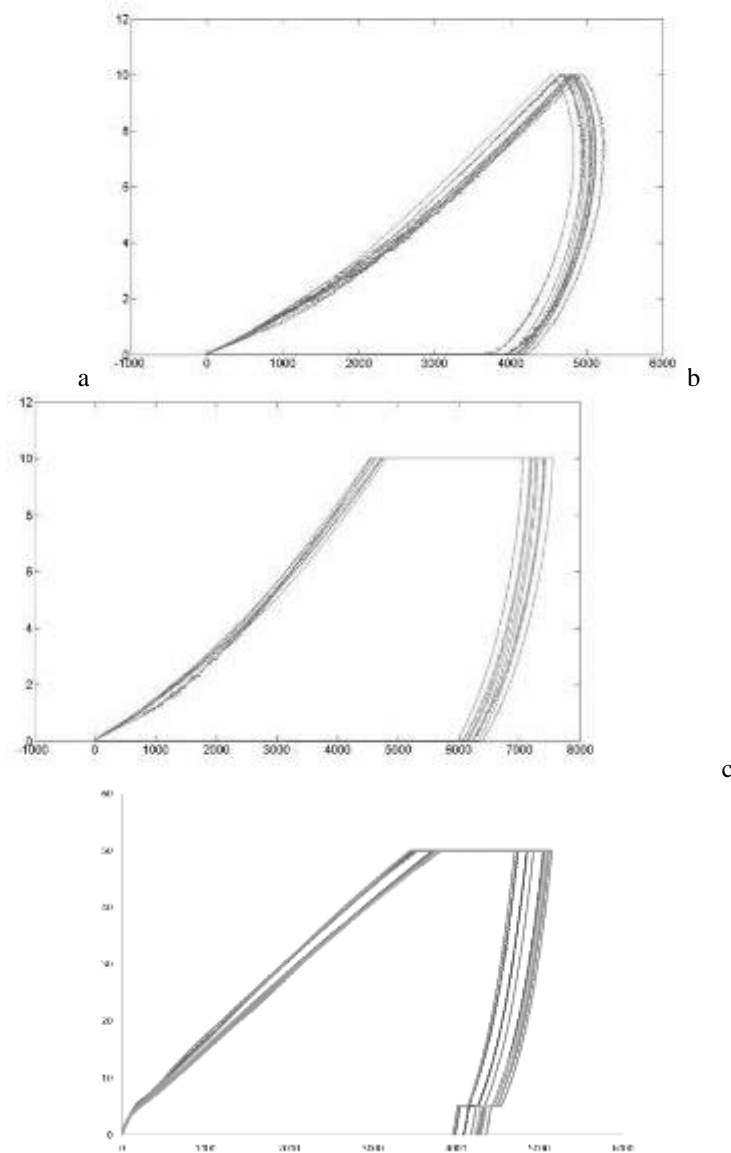| Indenter	h_{max}, nm	h_c, nm	P_{max}, mN	N, Mpa	E_r, GPa	E_s, GPa	C, nm/ mN
Berkovich	6121 (129)	580 2 (12 4)	10 (0.0)	12.5 (0.5)	0.715 (0.028)	0.6 4	42.5 (1)
Spherical	4839 (90)	450 9 (79)	50 (0.0)	227 (2.8)	6.8 (0.27)	6.1	8.8 (0.3)

Fig. 2. Loading diagram (along the horizontal axis - displacement of the indenter, along the vertical axis - load). a: without withstanding maximum load, Berkovich indenter, (b) with maximum load withstanding 100 s, Berkovich indenter, (c) with maximum load (100 s), spherical indenter.

In the course of the experiment on nanoindentation on the load - deformation relationship, it was found that the deformation continues to grow with decreasing load. At the same time, on the load-deformation curve during unloading, we observe a bend characteristic of polymer materials (Fig. 2a), which characterizes the viscoelastic properties of polymers. To avoid the influence of this effect on the result of determining the mechanical characteristics of the coating, it is necessary to withstand the sample for a rather long time at the maximum load. During this time, under a constant load, the deformation reaches its maximum value, and relaxation processes take place in the polymer. After that, the unloading curve will take a flat shape, acceptable for determining the elastic properties by the Oliver-Pharr method.

In the course of the experiment, it was found that when using the Berkovich indenter, the identified properties are extremely low in comparison with the known macroscopic characteristics. Thus, the value of the calculated Young's modulus of the coating turns out to be 0,64 GPa, which is five times lower than the known data from the macro experiment (3 GPa). In the case of using the Berkovich indenter, the result with respect to the Young's modulus of the coverage turns out to be overestimated and amounts to 6,1 GPa, which can be explained by the fact that the Oliver-Pharr model does not work well enough for the selected test mode, and it is probably necessary to use other approaches to identify Young's modulus of the cover. For example, it is possible to refine the data obtained by direct numerical simulation of the indentation process taking into account the nonlinear properties of

the coating and the contact parameters. Such modeling is planned to be carried out in the course of subsequent research.

4. Conclusions

The results of the tests carried out indicate the effectiveness of using the nanoindentation method for assessing the mechanical properties of paint and varnish coatings. However, the data obtained allow us to speak of a significant influence of the indenter shape on the measurement results. The use of an indenter in the Berkovich shape is apparently unjustified, since the pointed apex of the pyramid damages or cuts the coating surface, which leads to underestimated elastic properties. The use of a spherical indenter is more justified, since in this case there is no damage to the material surface. However, the found values of elastic properties seem to be overestimated when compared with the known data from macroexperiments and with typical values for the studied class of polymers. For a more accurate identification of the elastic properties of the coating based on the simulation results, it seems necessary to carry out a direct numerical simulation of the nanoindentation process.

References

1. Kuznetsova, E.L., Makarenko, A.V. Mathematical model of energy efficiency of mechatronic modules and power sources for prospective mobile objects // Periodico Tche Quimica, 2019, 16 (32), p. 529–541.
2. Rabinskii, L.N., Tushavina, O.V. Composite Heat Shields in Intense Energy Fluxes with Diffusion// Russian Engineering Research, 2019, 39(9), p. 800–803.
3. Rabinskiy, L.N., Tushavina, O.V. Investigation of the influence of thermal and climate effects on the performance of tiled thermal protection of spacecraft//Periodico Tche Quimica, 2019, 16(33), p. 657–667.
4. Bodryshev V. V., Rabinskiy L.N., Nartova L.G., Korzhov N.P. Geometry analysis of supersonic flow around two axially symmetrical bodies using the digital image processing method // Periódico Tchê Química. 2019. vol. 16, no. 33, pp. 541-548.
5. Formalev, V.F., Kolesnik, S.A., Kuznetsova, E.L. Analytical study on heat transfer in anisotropic space with thermal conductivity tensor components depending on temperature//Periodico Tche Quimica, 2018, 15(Special Issue 1), p. 426–432.
6. Formalev, V.F., Kolesnik, S.A. Temperature-dependent anisotropic bodies thermal conductivity tensor components identification method// International Journal of Heat and Mass Transfer, 2018, 123, p. 994–998.
7. Formalev, V.F., Kolesnik, S.A., Kuznetsova, E.L. Analytical solution-based study of the nonstationary thermal state of anisotropic composite materials // Composites: Mechanics, Computations, Applications. 2018. 9(3), p. 223-237.
8. Formalev, V.F., Kolesnik, S.A. On Thermal Solitons during Wave Heat Transfer in Restricted Areas // High Temperature, 2019, 57(4), p. 498–502.
9. Formalev, V.F., Kolesnik, S.A., Kuznetsova, E.L., Rabinskiy, L.N. Origination and propagation of temperature solitons with wave heat transfer in the bounded area during additive technological processes // Periodico Tche Quimica. 2019. 16(33), p. 505-515.
10. Formalev, V.F., Kolesnik, S.A., Kuznetsova, E.L. Mathematical modeling of a new method of thermal protection based on the injection of special coolants // Periodico Tche Quimica. 2019.16(32), p. 598-607.
11. Formalev, V.F., Kolesnik, S.A. On Inverse Coefficient Heat-Conduction Problems on Reconstruction of Nonlinear Components of the Thermal-Conductivity Tensor of Anisotropic Bodies // Journal of Engineering Physics and Thermophysics. 2017. 90(6), p. 1302-1309.
12. Formalev, V.F., Kolesnik, S.A. Analytical investigation of heat transfer in an anisotropic band with heat fluxes assigned at the boundaries // Journal of Engineering Physics and Thermophysics. 2016. 89(4), p. 975-984.
13. Formalev, V.F., Kartashov, É.M., Kolesnik, S.A. Simulation of Nonequilibrium Heat Transfer in an Anisotropic Semispace Under the Action of a Point Heat Source// Journal of Engineering Physics and Thermophysics. 2019. 92(6), p. 1537-1547.
14. I.S. Kurchatov, N.A. Bulychev, S.A. Kolesnik. Obtaining Spectral Characteristics of Semiconductors of AIIBVI Type Alloyed with Iron Ions Using Direct Matrix Analysis, International Journal of Recent Technology and Engineering, 2019, Vol. 8, I. 3, p. 8328-8330.

15. Formalev, V.F., Kolesnik, S.A., Kuznetsova, E.L. Identification of new law for decomposition of bonding heat-shielding composite materials/Asia Life Sciences. 2019. (1), p. 139-148.

16. Rabinskiy, L.N., Kuznetsova, E.L. Analytical and numerical study of heat and mass transfer in composite materials on the basis of the solution of a stefan-type problem// Periodico Tche Quimica, 2018, 15 (Special Issue 1), p. 339–347.

17. Bulychev, N.A., Kuznetsova, E.L. Ultrasonic Application of Nanostructured Coatings on Metals// Russian Engineering Research, 2019, 39 (9), p. 809–812.

18. Bulychev, N.A., Bodryshev, V.V., Rabinskiy, L.N. Analysis of geometric characteristics of two-phase polymer-solvent systems during the separation of solutions according to the intensity of the image of micrographs//Periodico Tche Quimica, 2019, 16(32), p. 551–559.

19. Formalev, V.F., Kartashov, É.M., Kolesnik, S.A. On the Dynamics of Motion and Reflection of Temperature Solitons in Wave Heat Transfer in Limited Regions // Journal of Engineering Physics and Thermophysics, 2020, 93(1), p. 10–15.

20. Formalev, V.F., Bulychev, N.A., Kuznetsova, E.L., Kolesnik, S.A. The Thermal State of a Packet of Cooled Microrocket Gas-Dynamic Lasers // Technical Physics Letters, 2020, 46(3), p. 245–248.

21. Rabinskiy, L.N., Tushavina, O.V., Formalev, V.F. Mathematical modeling of heat and mass transfer in shock layer on dimmed bodies at aerodynamic heating of aircraft// Asia Life Sciences, 2019, (2), p. 897–911.

22. Antufev, B.A., Egorova, O.V., Rabinskiy, L.N. Quasi-static stability of a ribbed shell interacting with moving load// INCAS Bulletin, 2019, 11, p. 33–39.

23. Bodryshev, V.V., Babaytsev, A.V., Rabinskiy, L.N. Investigation of processes of deformation of plastic materials with the help of digital image processing// Periodico Tche Quimica, 2019, 16(33), p. 865–876.

24. Astapov, A.N., Kuznetsova, E.L., Rabinskiy, L.N. Operating capacity of anti-oxidizing coating in hypersonic flows of air plasma // Surface Review and Letters, 2019, 26(2), 1850145 p.

25. Rabinskiy, L.N., Tushavina, O.V., Starovoitov, E.I. Study of thermal effects of electromagnetic radiation on the environment from space rocket activity // INCAS Bulletin, 2020, 12 (Special Issue), p. 141–148.

26. Babaytsev, A.V., Orekhov, A.A., Rabinskiy, L.N. Properties and microstructure of AlSi10Mg samples obtained by selective laser melting// Nanoscience and Technology: An International Journal, 2020, 11(3), p. 213–222.

27. Egorova, O.V., Kyaw, Y.K. Solution of inverse non-stationary boundary value problems of diffraction of plane pressure wave on convex surfaces based on analytical solution//Journal of Applied Engineering Science, 2020, 18(4), p. 676–680.

28. Rabinskiy, L.N., Sitnikov, S.A. Development of technologies for obtaining composite material based on silicone binder for its further use in space electric rocket engines// Periodico Tche Quimica, 2018, 15(Special Issue 1), p. 390–395.

29. M.O. Kaptakov. Effect of Ultrasonic Treatment on Stability of TiO2 Aqueous Dispersions in Presence of Water-Soluble Polymers, International Journal of Pharmaceutical Research, 2020, Vol. 12, Supplementary Issue 2, pp. 1821-1824.

30. O.A. Butusova. Surface Modification of Titanium Dioxide Microparticles Under Ultrasonic Treatment, International Journal of Pharmaceutical Research, 2020, Vol. 12, I. 4, pp. 2292-2296.

31. Bulychev N. A., Kuznetsova E.L., Bodryshev V. V. Rabinskiy L.N. Nanotechnological aspects of temperature-dependent decomposition of polymer solutions, Nanoscience and Technology: An International Journal, 2018, Vol. 9 (2), p. 91-97.

32. Bulychev, N.A., Rabinskiy, L.N. Ceramic nanostructures obtained by acoustoplasma technique//Nanoscience and Technology: An International Journal, 2019, 10 (3), p. 279–286.

33. Yu.V. Ioni. Nanoparticles of noble metals on the surface of graphene flakes, Periodico Tche Quimica, 2020, Vol. 17, No. 36, pp. 1199-1211.

34. Anikin V.A., Vyshinsky V.V., Pashkov O.A., et al. Using the maximum pressure principle for verification of calculation of stationary subsonic flow. Herald of the Bauman Moscow State Technical University, Series Mechanical Engineering, 2019, no. 6, pp. 4–16.

35. Bulychev, N.A., Rabinskiy, L.N., Tushavina, O.V. Effect of intense mechanical vibration of ultrasonic frequency on thermal unstable low-temperature plasma// Nanoscience and Technology: An International Journal, 2020, 11 (1), p. 15–21.

36. O.A. Butusova. Vinyl Ether Copolymers as Stabilizers of Carbon Black Suspensions, International Journal of Pharmaceutical Research, 2020, Vol. 12, Supplementary Issue 2, pp. 1152-1155.

37. Yu.V. Ioni. Effect of Ultrasonic Treatment on Properties of Aqueous Dispersions of Inorganic and Organic Particles in Presence of Water-Soluble Polymers, International Journal of Pharmaceutical Research, 2020, Vol. 12, Issue 4, pp. 3440-3442.

38. O.A. Butusova. Adsorption Behaviour of Ethylhydroxyethyl Cellulose on the Surface of Microparticles of Titanium and Ferrous Oxides, International Journal of Pharmaceutical Research, 2020, Vol. 12, Supplementary Issue 2, pp. 1156-1159.

39. A.N. Tarasova. Vibration-based Method for Mechanochemical Coating Metallic Surfaces, International Journal of Pharmaceutical Research, 2020, Vol. 12, Supplementary Issue 2, pp. 1160-1168.

40. Yu.V. Ioni, A. Ethiraj. New Tailor-Made Polymer Stabilizers for Aqueous Dispersions of Hydrophobic Carbon Nanoparticles, International Journal of Pharmaceutical Research, 2020, Vol. 12, Issue 4, pp. 3443-3446.

41. O.A. Butusova. Stabilization of Carbon Microparticles by High-Molecular Surfactants, International Journal of Pharmaceutical Research, 2020, Vol. 12, Supplementary Issue 2, pp. 1147-1151.

42. M.O. Kaptakov. Enhancement of Quality of Oil Products under Ultrasonic Treatment, International Journal of Pharmaceutical Research, 2020, Vol. 12, Supplementary Issue 2, pp. 1851-1855.

43. Yu.V. Ioni. Synthesis of Metal Oxide Nanoparticles and Formation of Nanostructured Layers on Surfaces under Ultrasonic Vibrations, International Journal of Pharmaceutical Research, 2020, Vol. 12, Issue 4, pp. 3432-3435.

44. A.N. Tarasova. Effect of Vibration on Physical Properties of Polymeric Latexes, International Journal of Pharmaceutical Research, 2020, Vol. 12, Supplementary Issue 2, pp. 1173-1180.

45. Potential Measuring, International Journal of Pharmaceutical Research, 2020, Vol. 12, Issue 4, pp. 3436-3439.

46. N.A. Bulychev, M.A. Kazaryan. Optical Properties of Zinc Oxide Nanoparticles Synthesized in Plasma Discharge in Liquid under Ultrasonic Cavitation, Proceedings of SPIE, 2019, Vol. 11322, article number 1132219.

47. Yu.V. Ioni, A. Ethiraj. Study of Microparticles Surface Modification by Electrokinetic A.N. Tarasova. Effect of Reagent Concentrations on Equilibria in Water-Soluble Complexes, International Journal of Pharmaceutical Research, 2020, Vol. 12, Supplementary Issue 2, pp. 1169-1172.

48. N.A. Bulychev, A.V. Ivanov. Effect of vibration on structure and properties of polymeric membranes, International Journal of Nanotechnology, 2019, Vol. 16, Nos. 6/7/8/9/10, pp. 334 – 343.

49. M.O. Kaptakov. Catalytic Desulfuration of Oil Products under Ultrasonic Treatment, International Journal of Pharmaceutical Research, 2020, Vol. 12, Supplementary Issue 2, pp. 1838-1843.

50. N.A. Bulychev, A.V. Ivanov. Nanostructure of Organic-Inorganic Composite Materials Based on Polymer Hydrogels, International Journal of Nanotechnology, 2019, Vol. 16, Nos. 6/7/8/9/10, pp. 344 – 355.

51. N.A. Bulychev, A.V. Ivanov. Study of Nanostructure of Polymer Adsorption Layers on the Particles Surface of Titanium Dioxide, International Journal of Nanotechnology, 2019, Vol. 16, Nos. 6/7/8/9/10, pp. 356 – 365.